Aerial Reconnaissance and Ground Robot Terrain Learning in Traversal Cost Assessment

Miloš Prágr[0000−0002−8213−893X]*, Petr Váňa[0000−0003−2155−5788], and Jan Faigl[0000−0002−6193−0792]

Faculty of Electrical Engineering, Czech Technical University in Prague,
Technicka 2, 166 27, Prague, Czech Republic
{pragrmi1,vanapet1,faiglj}@fel.cvut.cz
https://comrob.fel.cvut.cz

Abstract. In this paper, we report on the developed system for assessment of ground unit terrain traversal cost using aerial reconnaissance of the expected mission environment. The system combines an aerial vehicle with ground robot terrain learning in the traversal cost modeling utilized in the mission planning for ground units. The aerial vehicle is deployed to capture visual data used to build a terrain model that is then used for the extraction of the terrain features of the expected operational area of the ground units. Based on the previous traversal experience of the ground units in similar environments, the learned model of the traversal cost is employed to predict the traversal cost of the new expected operational area to plan a cost-efficient path to visit the desired locations of interest. The particular modules of the system are demonstrated in an experimental scenario combining the deployment of an unmanned aerial vehicle with a multi-legged walking robot used for learning the traversal cost model.

1 Introduction

Mobile robots deployed in outdoor environments can encounter hard-to-traverse areas which may hinder their motion efficiency and thus impede their assigned missions. Therefore, the traversability of the encountered terrains should be taken into account during mission planning to avoid parts of the environment with difficult terrains. Such terrain evaluation systems may entice the robot to avoid certain terrain types which have been learned from human labels [2], evaluate terrain geometry to avoid rough areas [18], or tradeoff the robot safety with the predicted execution time [3].

In [13], the traversal cost learning has been proposed based on the proprioceptive traversal cost experienced by the robot that is combined with the terrain appearance and geometry captured by the robot. A deployment of the terrain traversal cost learning and cost prediction has been reported within a path planning scenario [14] and an autonomous exploration mission [12]. On the other hand, mission planning can take advantage of the overhead imagery of the operational area, e.g., using an Unmanned Aerial Vehicle (UAV). The authors of [8]

use a convolutional neural network on the RGB aerial imagery to classify terrains from the Estonian Land Board database. In [16], HSV locale-specific overhead features are used to predict LADAR-based features characterizing ground unit traversability. Kohonen's Self-organizing Maps [9] are used in [4] to identify potential invasion, unauthorized changes of land, and deforestation. Finally, overhead imagery has also been deployed in various disaster scenarios. The authors of [15] develop a UAV to map landslides; and in [17], a road network-based feature is used to localize aerial platforms over areas altered by earthquakes where previously available landmarks may be missing.

In this paper, we consider overhead imagery to facilitate energy-efficient multi-goal path planning for ground units represented by a small hexapod walking robot operating in an outdoor environment. A UAV is utilized to capture the outdoor field environment, and the RGB overhead imagery is coupled with the proprioceptive experience of the small hexapod walking robot. The Locally Weighted Projection Regression (LWPR) [19] is used to predict energy-based traversal cost from the overhead data. The traversal cost model is then coupled with the Traveling Salesman Problem (TSP) solver to find the energy-efficient multi-goal path to visits all the assigned goals.

The rest of the paper is organized as follows. The problem of multi-goal path planning from aerial imagery is presented in Section 2. The proposed methodology for prediction of ground unit traversal cost from overhead imagery and its use in multi-goal path planning is presented in Section 3. The experimental deployment scenario with the aerial imagery and ground robot proprioception dataset are described in Section 4. Finally, the paper is concluded in Section 5.

2 Multi-goal Path Planning from Aerial Imagery

The overhead imagery is utilized to facilitate energy-efficient multi-goal path planning for a ground unit, which is represented by a small hexapod walking robot shown in Fig. 1a. The robot is requested to visit a set of goal locations and return to its starting position that is the multi-goal path planning problem that can be formulated as the TSP [1]. The TSP is a well-studied problem formulation with several existing approaches [5]; however, we need to determine the individual costs of traveling from one goal location to another location. In this work, we consider the traversal cost assessment based on the learned terrain model as follows.

The prior experience with traversing various terrains is employed to select a path that minimizes the overall energy exertion. The environment is represented as a grid which corresponds to the overhead RGB image of the mission location, such as the area shown in Fig 1b.

The robot proprioceptive experience is represented by the robot power consumption measurements, where the instantaneous power consumption [10] is

$$P_{in} = V \cdot I \quad [\mathrm{W}], \tag{1}$$

where V is the current battery voltage, and I is the instantaneous current measurement sampled with 200 Hz. Due to the sampling, we can represent the time

(a) Hexapod walking robot (b) RGB overhead image

Fig. 1. The (a) hexapod walking robot and (b) overhead image of the mission area.

interval T as a sequence of n time stamps $T = (t_1, \ldots, t_n)$. The energy consumption over T can be then computed as

$$E(T) = \sum_{i=1}^{n-1} (t_i - t_{i-1}) \frac{P_{in}(t_{i-1}) + P_{in}(t_i)}{2} \quad [\mathrm{J}], \tag{2}$$

where t_i and t_{i-1} represent time stamps of two consecutive power consumption measurements. Finally, the robot traversal cost experience over the time interval T is the power consumption per distance traveled over the duration of T and can be defined as

$$c(T) = \frac{E(T)}{d(T)} \quad [\mathrm{Jm}^{-1}], \tag{3}$$

where $d(T)$ is the distance traveled by the robot over the interval T.

In the presented results, we solve the instances of the TSP by the LKH solver [6] since it is known to be a fast heuristic providing a solution close to the optimum. However, in comparison to optimal solvers, the asymptotic time complexity of the LKH solver can be bounded by $\mathcal{O}(n^{2.2})$, which is sufficient even for quick updates of mission plans with tens of goal locations.

The TSP solver utilizes the distance matrix D where each element $D_{i,j}$ represents the energy exertion needed to travel from the location i to the location j. Therefore, the needed energy is determined as the path planning problem to find a path P^* from the corresponding grid cell n_g to the desired cell n'_g with the minimal energy exertion $E(P^*)$ as

$$P^* = \mathrm{argmin}_P \, E(P) = \mathrm{argmin}_P \sum_{i=1}^{|P|-1} E(n_i, n_{i+1}) \text{ with } n_1 = n_g, n_{|P|} = n'_g \tag{4}$$

where the path P is as a sequence of grid cells $P = (n_1, ..., n_{|P|})$, $|P|$ is the number of cells of the path P, and $E(n_i, n_j)$ is the energy to traverse from the grid cell n_i to n_j in its 8-neighborhood that is computed as

$$E(n_i, n_j) = \|(n_i, n_j)\| c_{model}(n_i, n_j) \quad [\mathrm{J}], \tag{5}$$

where $\|(n_i, n_j)\|$ is the Euclidean distance between n_i and n_j; and $c_{model}(n_i, n_j)$ is the traversal cost prediction to traverse from n_i to n_j. The cost learning and prediction is further detailed in the following section.

3 Proposed method

In this section, we describe how the overhead imagery is used to learn the model of the traversal cost that is utilized in the robot energy-efficient path planning according to (5). First, the overhead image of the mission environment is transformed into feature descriptors of the terrain by applying the Gaussian blur filter with $\Sigma = \lambda I$, where the parameter $\lambda = 5$ is selected with regards to the overhead image resolution. Thus, a particular terrain appearance descriptor $\boldsymbol{d}_t = (r, g, b)$ is defined as the RGB colors at the terrain's respective coordinates (pixels) in the blurred image. Then, such a particular terrain appearance descriptor is utilized either for the traversal cost learning; or traversal cost assessment. For the cost learning, the terrain descriptor is paired with the robot experience to learn the traversal cost model. For the cost assessment, the descriptor of a priory untraversed terrain is used with the model to predict the traversal cost, and thus the energy exertion over such terrain.

The experienced traversal cost is computed according to (3) for 10 s long intervals, which roughly span the gait cycle duration of the utilized hexapod walking robot. The intervals are then manually paired with the robot trajectory in the overhead image. Thus, each interval is assigned a terrain descriptor $\boldsymbol{d}_t$, which is combined with the experienced cost c to create the experience descriptor $\boldsymbol{d}_c = (r, g, b, c)$. The traversal cost model is learned by the LWPR algorithm [19] from a random permutation of the training set that consists of the terrain descriptors accompanied by the recorded traversal cost. The learning is repeated 10 times. The LWPR is parametrized with the initial distance metric $\mathbf{D}_{\text{init}} = 10\mathbf{I}$ and the distance metric learning rate $\alpha_{\text{init}} = 10$.

A priory unknown traversal cost c^* for a particular terrain descriptor d_t can be then predicted as

$$c^* = c_{LWPR}(\boldsymbol{d}_t). \tag{6}$$

Further, the traversal cost prediction $c_{model}(n_i, n_j)$ to traverse from the grid cell n_i to its neighbor n_j is defined as the mean of the LWPR predictions at the two respective grid cells

$$c_{model}(n_i, n_j) = \frac{c_{LWPR}(\boldsymbol{d}_t(n_i)) + c_{LWPR}(\boldsymbol{d}_t(n_j))}{2}, \tag{7}$$

where $d_t(n)$ is the terrain descriptor corresponding to the grid cell n.

4 Results

The proposed approach has been experimentally verified in the outdoor environment shown in Fig. 1b. The resolution of the used overhead image is 960×544 pixels. The Python bindings of the LWPR implementation [11] have been utilized

to compute the LWPR models, and the available implementation of the LKH [7] has been used to solve instances of the TSP. The hexapod walking robot has traversed four different terrains; see Fig. 2. Every terrain has been traversed in at least three trials, each few gait cycles long. The *concrete* and *gravel* terrains are relatively easy to traverse, and the robot exhibits the lowest traversal cost. The *grass* is harder to traverse, and the cost is high. Finally, when traversing the *vegetation*, the robot is almost stuck and moves very slowly. Therefore, the traversal cost over the *vegetation* is the highest. In total, the learning set comprises 1094 traversal cost measurements paired with terrain descriptors. On average, it takes is 2.31 s (the wall time determined as the mean of 10 trials) to learn the LWPR model using the Intel Core i5-4460 CPU with 16 GB memory. The mean time to predict the traversal costs for the whole 960×544 pixel overhead image is 1.82 s.

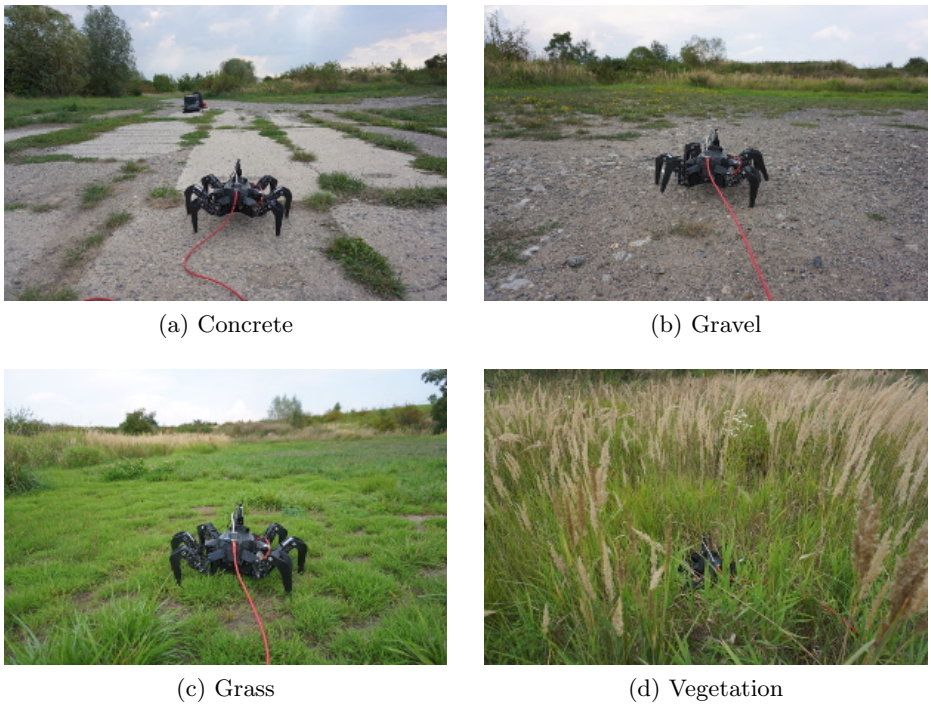

(a) Concrete (b) Gravel

(c) Grass (d) Vegetation

Fig. 2. The hexapod walking robot traversing various terrains during the experimental deployment.

The approach is tested in three scenarios over the same mission area to demonstrate solutions with a different number of goal locations. In *Scenario 1*, the robot needs to plan a visit of 10 locations, which are mostly selected near, but not necessarily on, areas labeled as easily traversable according to human expertise. In *Scenario 2*, 10 points are spaced more evenly over the mission area.

Finally, 42 locations need to be visited in *Scenario 3*. The LKH solutions for *Scenarios 1*, *2*, and *3* are computed in 0.12 s, 0.12 s, and 0.25 s, respectively.

The traversal cost predictions and the paths computed for the individual scenarios are projected onto the overhead image, see Fig. 3, Fig. 4, and Fig. 5. Notice, even though the same learning set is used in each scenario, each time the traversal cost model is relearned with a different random permutation of the dataset to show an effect of the traversal cost learning which depends not only on the available learning data but also on the learning procedure itself. Thus, the predicted traversal costs slightly differ in the individual scenarios; however, the overall course of the planned path follows the rough distinction between the hard and easy to traverse terrains.

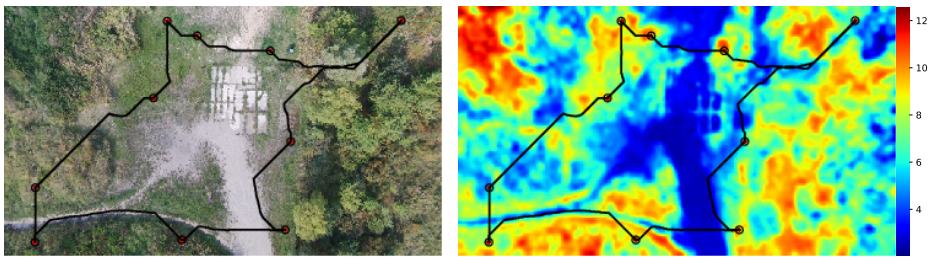

(a) RGB (b) Cost prediction

Fig. 3. The planned path in *Scenario 1* projected onto the overhead image.

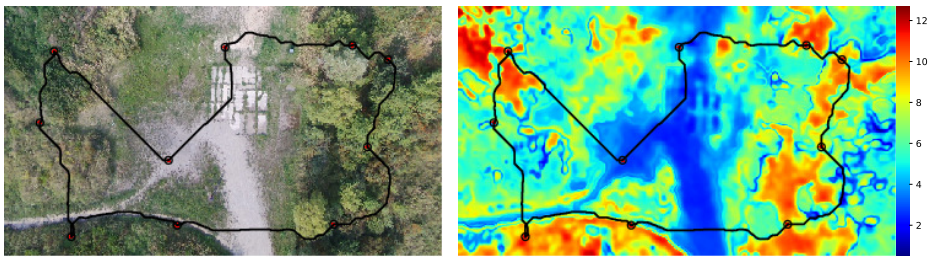

(a) RGB (b) Cost prediction

Fig. 4. The planned path in the *Scenario 2* projected onto the overhead image.

In *Scenario 1* and *Scenario 2*, the computed paths often follow the concrete and gravel terrains, as these are the most energetically efficient terrain types. However, in some instances, the robot may choose to plan over the rougher terrain if such a path is significantly shorter despite higher traversal cost. In

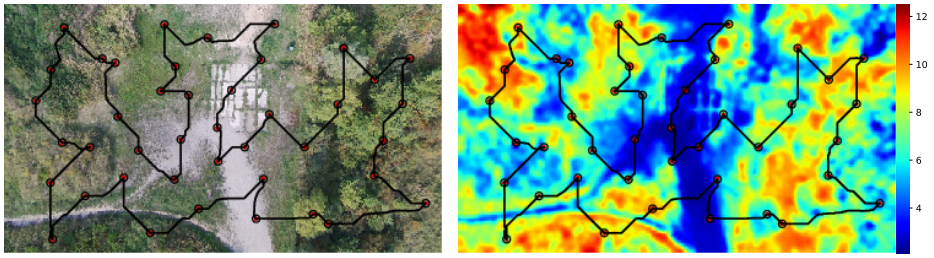

(a) RGB (b) Cost prediction

Fig. 5. The planned path in the *Scenario 3* projected onto the overhead image.

Scenario 3, the effect of traversal cost is much less prevalent because the higher density of points forces the robot to visit virtually every available terrain type. Regardless, even in this case, the path seems to avoid the rough areas to a lesser extent.

5 Conclusion

In this paper, overhead imagery is combined with traversal cost learning to predict energy-based traversal cost of the multi-goal path in an outdoor mission with a hexapod walking robot. The traversal cost model that predicts the energy exerted per meter from RGB features in overhead imagery is learned using the LWPR algorithm. The proposed system is experimentally verified in an outdoor scenario using a small UAV and hexapod walking robot. The herein presented results support the feasibility of the proposed approach and suggest that the approach has been deployed successfully. In our future work, we aim to extend the presented approach to online learning using real-time communication between the ground and aerial vehicles.

Acknowledgement

The presented work has been supported under the OP VVV funded project CZ.02.1.01/0.0/0.0/16_019/0000765 “Research Center for Informatics”. The support under grant No. SGS19/176/OHK3/3T/13 to Miloš Prágr and Petr Váňa is also gratefully acknowledged.

References

1. Alatartsev, S., Stellmacher, S., Ortmeier, F.: Robotic Task Sequencing Problem: A Survey. Journal of Intelligent & Robotic Systems **80**(2), 279–298 (2015). DOI: 10.1007/s10846-015-0190-6

2. Belter, D., Wietrzykowski, J., Skrzypczyński, P.: Employing Natural Terrain Semantics in Motion Planning for a Multi-Legged Robot. Journal of Intelligent & Robotic Systems **93**(3), 723–743 (2019). DOI: 10.1007/s10846-018-0865-x
3. Brunner, M., Brüggemann, B., Schulz, D.: Rough Terrain Motion Planning for Actuated, Tracked Robots. In: International Conference on Agents and Artificial Intelligence (ICAART). pp. 40–61. Springer (2013). DOI: 10.1007/978-3-662-44440-5_{}3
4. Felizardo, L.F., Mota, R.L., Shiguemori, E.H., Neves, M.T., Ramos, A.B., Mora-Camino, F.: Using ANN and UAV for terrain surveillance. In: International Conference on Hybrid Intelligent Systems (HIS). pp. 1–5 (2014). DOI: 10.1109/HIS.2013.6920414
5. Gutin, G., Punnen, A.P. (eds.): The Traveling Salesman Problem and Its Variations. Springer US (2007). DOI: 10.1007/b101971
6. Helsgaun, K.: An Effective Implementation of the Lin-Kernighan Traveling Salesman Heuristic. European Journal of Operational Research **126**(1), 106–130 (2000)
7. Helsgaun, K.: LKH solver 2.0.9. http://www.akira.ruc.dk/~keld/research/LKH, http://www.akira.ruc.dk/~keld/research/LKH/, cited on 2019-08-29
8. Hudjakov, R., Tamre, M.: Aerial imagery terrain classification for long-range autonomous navigation. In: International Symposium on Optomechatronic Technologies. pp. 88–91 (2009). DOI: 10.1109/ISOT.2009.5326104
9. Kohonen, T.: The self-organizing map. Proceedings of the IEEE **78**(9), 1464–1480 (Sep 1990). DOI: 10.1109/5.58325
10. Kottege, N., Parkinson, C., Moghadam, P., Elfes, A., Singh, S.P.N.: Energetics-informed hexapod gait transitions across terrains. In: IEEE International Conference on Robotics and Automation (ICRA). pp. 5140–5147. IEEE (2015). DOI: 10.1109/ICRA.2015.7139915
11. LWPR library. https://github.com/jdlangs/lwpr (since 2007), cited on 2019-05-28
12. Prágr, M., Čížek, P., Bayer, J., Faigl, J.: Online Incremental Learning of the Terrain Traversal Cost in Autonomous Exploration. In: Robotics: Science and Systems (RSS) (2019). DOI: 10.15607/RSS.2019.XV.040
13. Prágr, M., Čížek, P., Faigl, J.: Cost of Transport Estimation for Legged Robot Based on Terrain Features Inference from Aerial Scan. In: IEEE/RSJ International Conference on Intelligent Robots and Systems (IROS). pp. 1745–1750 (2018). DOI: 10.1109/IROS.2018.8593374
14. Prágr, M., Čížek, P., Faigl, J.: Incremental Learning of Traversability Cost for Aerial Reconnaissance Support to Ground Units. In: 2018 Modelling & Simulation for Autonomous Systems (MESAS). pp. 412–421 (2019). DOI: 10.1007/978-3-030-14984-0_30
15. Rossi, G., Tanteri, L., Tofani, V., Vannocci, P., Moretti, S., Casagli, N.: Multitemporal UAV surveys for landslide mapping and characterization. Landslides **15**(5), 1045–1052 (2018). DOI: 10.1007/s10346-018-0978-0
16. Sofman, B., Lin, E., Bagnell, J.A., Cole, J., Vandapel, N., Stentz, A.: Improving Robot Navigation Through Self-Supervised Online Learning. Journal of Field Robotics **23**(11-12), 1059–1075 (2006). DOI: 10.1002/rob.20169
17. Soleimani, B., Ashtiani, M.Z., Soleimani, B.H., Moradi, H.: A Disaster Invariant Feature for localization. In: IEEE/RSJ International Conference on Intelligent Robots and Systems (IROS). pp. 1096–1101 (2010). DOI: 10.1109/IROS.2010.5651930

18. Stelzer, A., Hirschmüller, H., Görner, M.: Stereo-vision-based navigation of a six-legged walking robot in unknown rough terrain. International Journal of Robotics Research **31**(4), 381–402 (2012). DOI: 10.1177/0278364911435161
19. Vijayakumar, S., Schaal, S.: Locally Weighted Projection Regression : An O(n) Algorithm for Incremental Real Time Learning in High Dimensional Space. In: International Conference on International Conference on Machine Learning (ICML). pp. 1079–1086 (2000)